Diagenesis, low-grade and contact metamorphism in the Triassic-Jurassic of the Vichuquén-Tilicura and Hualañé-Gualleco Basins, Coastal Range of Chile

SCHWEIZ. MINERAL. PETROGR. MITT. 82, 375–392, 2002

Diagenesis, low-grade and contact metamorphism in the Triassic–Jurassic of the Vichuquén-Tilicura and Hualañé-Gualleco Basins, Coastal Range of Chile

by *Mauricio Belmar*[1], *Susanne Th. Schmidt*[2], *Rafael Ferreiro Mählmann*[3], *Josef Mullis*[3], *Willem B. Stern*[3] and *Martin Frey*[3] *(deceased)*

Abstract

Diagenetic and low-grade metamorphic conditions have been determined (pressure and temperature) for Late Triassic to Early Jurassic sedimentary rocks from the Vichuquén-Tilicura and the Hualañé-Gualleco basins in Central Chile using Kübler index (KI), coal rank data, K-white mica *b* cell dimension, characteristic mineral assemblages and fluid inclusion data. A burial-related diagenetic to low-grade metamorphic event, which is recorded in both basins, is partly overprinted in the Hualañé-Gualleco basin by contact metamorphism around Jurassic dioritic to granodioritic intrusions. Diagenetic conditions prevailed in the northern Vichuquén-Tilicura basin, whereas in the southern Hualañé-Gualleco basin low-grade metamorphism is observed with an increase in metamorphic grade from north to south. Epizonal conditions are locally reached in the very south of the Hualañé-Gualleco basin. Low-pressure conditions were determined using the K-white mica *b* cell dimension. A numerical maturity model corroborates with the regional low-grade metamorphism. Evidence of contact metamorphism in the immediate proximity of some Jurassic intrusions includes: (1) hornfels facies assemblages such as ferrosilite ($XFe_{0.6}$)-magnesiohornblende-ferroactinolite-biotite together with chlorite, plagioclase, stilpnomelane and (2) natural coke and pyrolitic bituminite in some sedimentary samples. Epizonal KI and high coal rank values are probably a result of this locally occurring contact metamorphism.

Keywords: diagenesis, low-grade metamorphism, contact metamorphism, illite crystallinity, K-white mica, coal rank.

Introduction

Low-grade metamorphism of mafic rocks in the Central Andes of Chile is probably one of the best documented examples of a depth-related increase of metamorphic grade from upper zeolite to greenschist facies (LEVI, 1969; AGUIRRE et al., 1978, 1997, 1999; LEVI et al., 1982; VERGARA et al., 1993). Mesozoic sedimentary rocks and intrusive igneous plutons are widespread in the coastal region south of Santiago but neither the metamorphic evolution nor the possible influence of contact metamorphism due to the presence of intrusive bodies have been studied. This study therefore aims to determine the P-T conditions and the influence of contact metamorphism in the Mesozoic sedimentary sequence in the Tilicura-Vichuquén and the Hualañé-Gualleco basins (between 34° 45' S and 35° 20' S or 100 km east of Curico and ca. 300 km south of Santiago de Chile) by applying several techniques: Kübler index (KI), coal rank, fluid inclusion microthermometry, identification of index minerals, critical mineral assemblages and thermal maturity modeling. Studies of low-grade metamorphism and related contact metamorphism in sedimentary rocks are relatively rare. NADEAU and REYNOLDS (1981) used the regional pattern of coal rank and the distribution of ordered versus random interstratification in illite/smectite in the Cretaceous Mancos

[1] Departamento de Geología, Universidad de Chile, Plaza Ercilla 803, casilla 13518, correo 21, Santiago, Chile. <mbelmar@ing.uchile.cl>
[2] Département de Minéralogie, Rue des Maraîchers 13, CH-1211 Genève, Switzerland. <susanne.schmidt@terre.unige.ch>
[3] Mineralogisch-Petrographisches Institut, Bernoullistrasse 30, CH-4056 Basel, Switzerland.

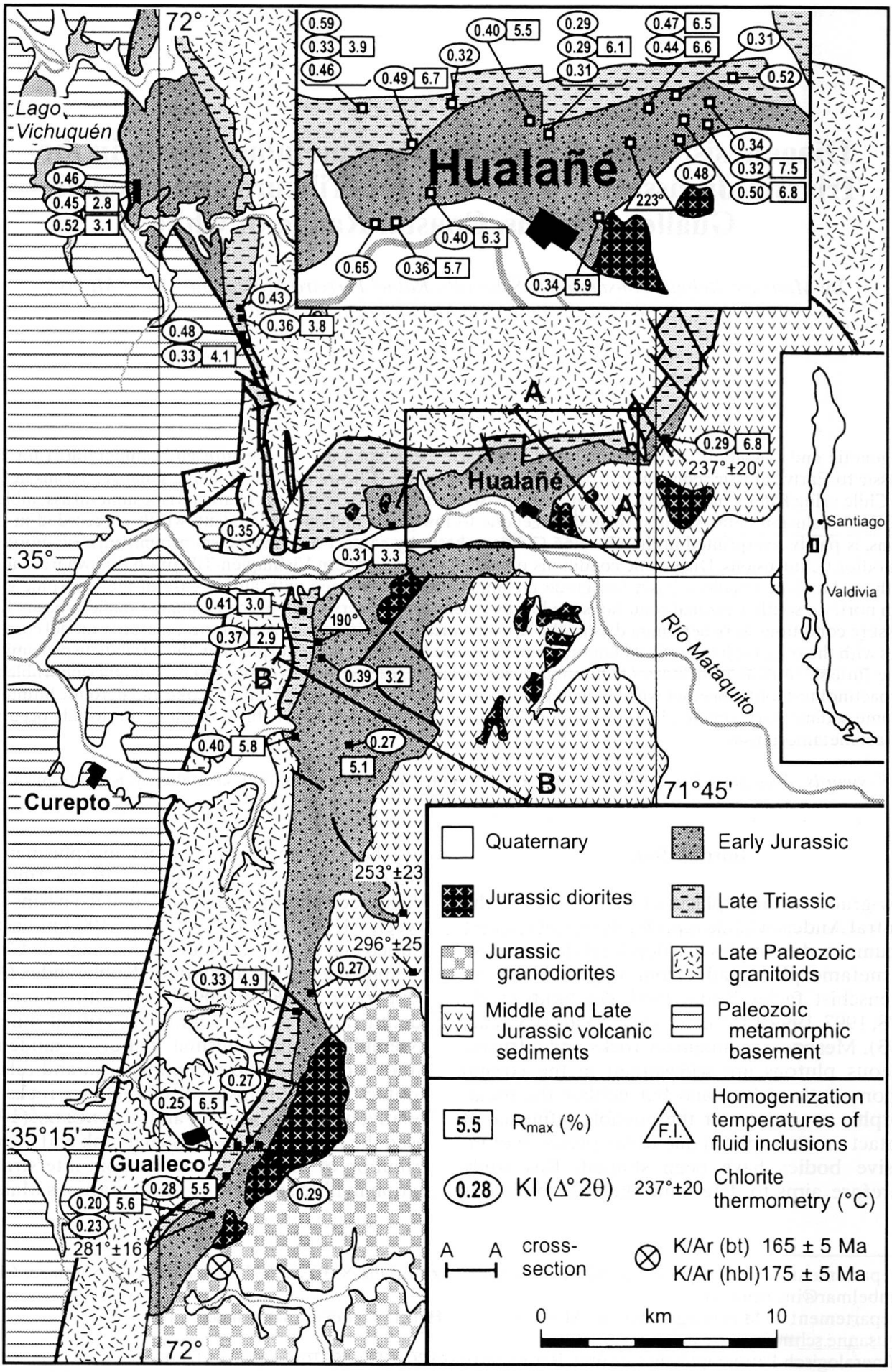
72°
Lago Vichuquén
Hualañé
0.59
0.33 3.9
0.46
0.49 6.7
0.32
0.40 5.5
0.29
0.29 6.1
0.31
0.47 6.5
0.44 6.6
0.31
0.52
0.34
0.32 7.5
0.48
0.50 6.8
223°
0.40 6.3
0.65
0.36 5.7
0.34 5.9
0.46
0.45 2.8
0.52 3.1
0.43
0.36 3.8
0.48
0.33 4.1
A
A
0.29 6.8
237°±20
Hualañé
0.35
35°
0.31 3.3
0.41 3.0
0.37 2.9
190°
B
0.39 3.2
0.40 5.8
0.27
5.1
B
Curepto
Rio Mataquito
71°45'
Santiago
Valdivia
253°±23
296°±25
0.27
0.33 4.9
0.27
0.25 6.5
35°15'
Gualleco
0.28 5.5
0.20 5.6
0.23
281°±16
0.29
72°
Quaternary
Early Jurassic
Jurassic diorites
Late Triassic
Jurassic granodiorites
Late Paleozoic granitoids
Middle and Late Jurassic volcanic sediments
Paleozoic metamorphic basement
5.5 Rmax (%)
F.I. Homogenization temperatures of fluid inclusions
0.28 KI (Δ°2θ)
237°±20 Chlorite thermometry (°C)
A A cross-section
K/Ar (bt) 165 ± 5 Ma
K/Ar (hbl) 175 ± 5 Ma
0 km 10

Shale of the southern Rocky Mountains and the Colorado Plateau to define the thermal regime of burial and contact metamorphism. HÉROUX and TASSÉ (1990) report that organic matter near alkaline intrusions in the St. Lawrence Lowlands in Quebec is characterized by mosaic textures and has higher reflectances than the background levels of organic matter in the dolostones of the Lower Ordovician Beckmantown Group. Based on Kübler index data, WARR et al. (1991) observed in the external Variscides of southwest England a coincidene between the areas of regional epizonal grade and the extent of a geophysically defined subsurface limit of a granite batholith. SACHSENHOFER et al. (1998) examined the southwestern basin of the Neogene Styrian basin, Slovenia, and the possible influence of Tertiary magmatic events on the maturation of organic matter. The present study reveals vitrinite anomalies which are related to the thermal overprinting by shallow plutons.

Geological setting

Late Triassic to Early Jurassic sedimentary rocks are exposed in the Vichuquén-Tilicura and the Hualañé-Gualleco basins (Fig. 1). They form part of an almost continuous belt of Mesozoic sedimentary rocks which is approximately 60 km in length and unconformably overlies the Paleozoic crystalline basement (Fig. 1). Tectonic development during the Triassic was controlled by continuous movements and differential uplift of the Paleozoic basement and lasted until at least the Jurassic (THIELE and MOREL, 1981). The western Paleozoic areas were exhumed at a faster rate than those to the east which preserve Mesozoic basin sedimentary rocks. The regional paleogeographic and tectono-sedimentary evolution during the Triassic–Jurassic resulted in a simple morphology characterized by basins and high structures (Figs. 1–2). Uplift of the western Paleozoic basement during the Triassic-Jurassic boundary resulted in the development of two sedimentary basins, known as the Vichuquén-Tilicura basin in the north and the Hualañé-Gualleco basin further to the southeast (Fig. 1). CORVALÁN (1976, 1994) mapped these two basins and established the general stratigraphy. He concluded that the rocks have only experienced diagenesis with the exception of local regions which have been contact metamorphosed by Jurassic granodiorites and diorites. The principal structures in the sedimentary strata are north-south fold axes and normal faults which are generally attributed to the rejuvenation of deep-seated structures in the Paleozoic basement. East-west faulting in the northern part of the Hualañé-Gualleco basin predates the prevailing NW–SE faulting (THIELE and MOREL, 1981; CORVALÁN, 1982). No cleavage is visible in the north, whereas an incipient cleavage has developed in the central and southern part of the Hualañé-Gualleco basin, indicating an increase in deformation towards the south.

The northern Vichuquén-Tilicura basin is 13 km long by 6 km wide and hosts the Lago de Vichuquén (Fig. 1). Late Triassic sedimentary rocks (CORVALÁN, 1976) are characterized by a marine sequence of lutites, shales and sandstones as well as volcanic and volcaniclastic sedimentary rocks (Fig. 3). Early Jurassic sedimentary rocks are in faulted contact with the Triassic rocks (Fig. 3) in the Lago de Vichuquén profile, and reach a mean thickness of 1250 m. They are predominantly composed of black fissile shales with minor sandstones and conglomerates (CORVALÁN, 1976, 1982). The western border of the Vichuquén-Tilicura basin (Figs. 1–2) is composed of a Paleozoic metamorphic basement sequence (GONZALES-BONORINO, 1970; MUNIZAGA et al., 1973; HERVÉ et al., 1982). In the northeastern part, the basin is limited by Late Paleozoic granitoid rocks. The Late Triassic to Early Jurassic sequence of mainly sedimentary rocks reaches a maximum thickness of up to 2600 m in the Hualañé-Gualleco basin and east of the village of Curepto (Figs. 1–3). In the eastern most part of the study area andesitic lava flows, volcanic breccias and sedimentary intercalations of Middle and Upper Jurassic are exposed (MOREL, 1981). The Jurassic intrusions are principally granodiorites, although they have dioritic borders (Fig. 1). GANA and HERVÉ (1983) published K/Ar ages of 165 ± 5 Ma (biotite) and 175 ± 5 Ma (hornblende) for these plutons.

Analytical methods

SAMPLE PREPARATION

Shales and slates were cleaned and their weathering rims were removed. They were subsequently ground in a disc mill for <40 s. Carbonate was removed using 5% acetic acid and the remaining material was washed with deionized water. The <2 μm fraction was obtained using settling tubes and

←*Fig. 1* Simplified geological map for the Lago Vichuquén-Hualañé-Gualleco areas, modified after CORVALÁN (1996) with the data of Kübler index (KI), coal rank (R_{max}), fluid inclusion (FI) and chlorite "geothermometry".

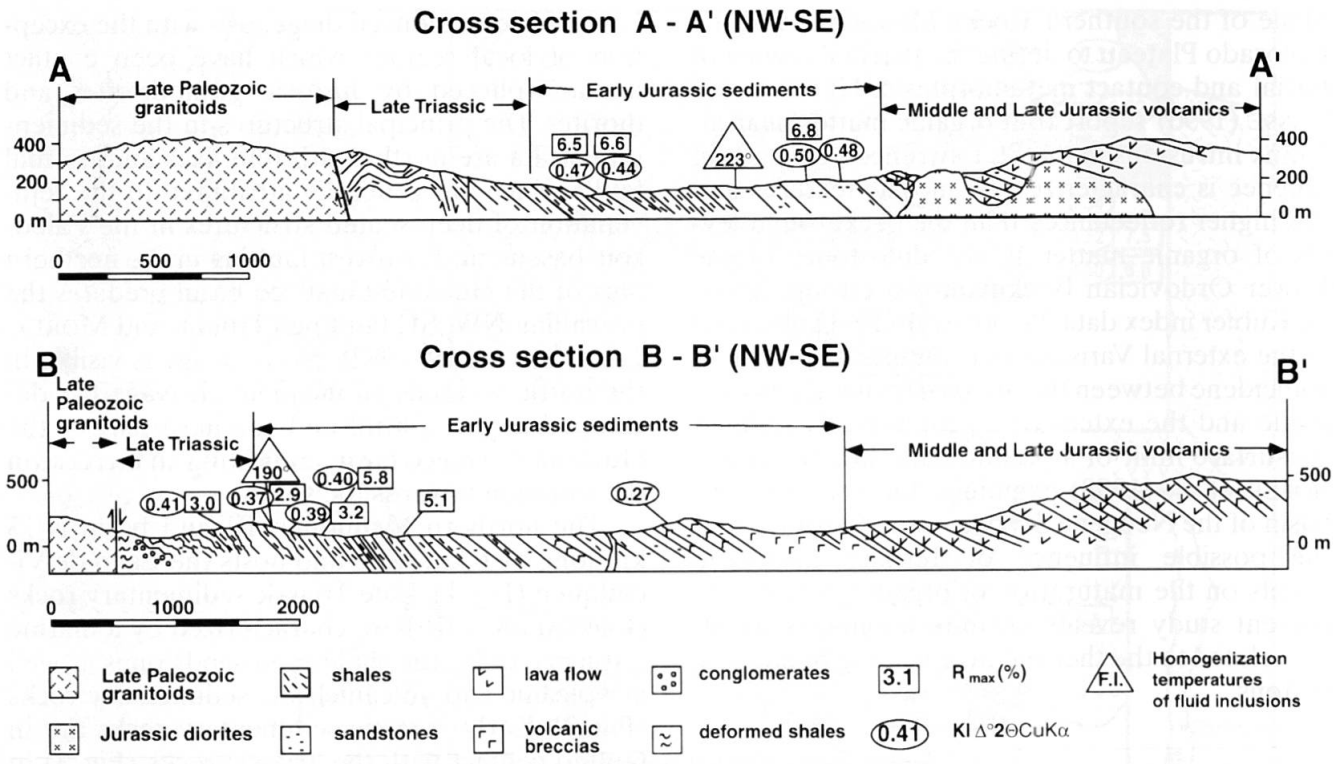

Fig. 2 Cross sections of the Hualañé-Gualleco basin. Cross section AA' shows increased R_{max} values as compared to KI values in the vicinity of Late Jurassic diorites. Cross section BB' shows KI and R_{max} values related to burial metamorphism.

Millipore© filters with a 0.1 μm pore size. The clay fraction was Ca-saturated with 2N $CaCl_2$. Oriented slides were prepared by pipetting the suspension onto glass slides (~5 mg cm^{-2}) and allowing it to air-dry. Glycolated mounts were prepared for smectite determination in a glycol steam bath at 60 °C overnight.

POWDER X-RAY DIFFRACTION

X-ray diffraction measurements were performed with a Siemens D-5000 diffractometer using the following instrumental settings: Cu Kα radiation, 40 kV, 30 mA; automatic primary and secondary divergence slits; secondary graphite monochromator. The goniometer settings for air-dried slides were: (i) 2–21 °2θ with a step increment of 0.05 °2θ and an integration time of 30 s, (ii) 21–42 °2θ with a step increment of 0.02 °2θ and an integration time of 1 s, (iii) 42–64 °2θ with a step increment of 0.02 °2θ and an integration time of 8 s. The goniometer settings for glycolated preparates were: 2–23 °2θ with a step increment of 0.03 °2θ and an integration time of 6 s. The scan speeds were: 0.1 °2θ min^{-1} for air-dried preparates with a total measuring time of 5.5 h and 0.33 °2θ min^{-1} for glycolated preparates with a total measuring time of 1.5 h. The d-spacing was calibrated against quartz occurring in the samples. The K-white mica *b* cell dimension was calculated from the (060, 331) spacing using the (211) quartz reflection as an internal standard. Randomly oriented powders with sizes <2 μm powders were used to eliminate the influence of detrital mica in larger size fractions. The samples were analyzed by step scanning from 59 to 63 °2θ to determine the (060, 331) interference.

KÜBLER INDEX

The Kübler index was determined as the angular peak width at half height of the first illite basal reflection (Kübler index, KI; KÜBLER 1967, 1984; GUGGENHEIM et al., 2002) on the 0.1–2.0 μm fraction, following the recommendations given by KISCH (1991). Measurements were performed on 49 samples of air-dried and glycolated preparates and calibrated following an interlaboratory standardization by DALLA TORRE and FREY (1997). Kübler index was not determined in samples yielding interferences of the first illite basal reflection with other phases, for example, paragonite or pyrophyllite. The limiting KI values for the low-grade and high-grade boundary of the anchizone are 0.42 and 0.25 Δ°2θ Cu Kα, respectively (FREY, 1987). The Δ°2θ standard deviation of KI values is ±0.02.

EXPANDABILITY AND ORDERING OF ILLITE/SMECTITE

The ordering and the percentage of illite in mixed-layer illite/smectite (I/S) were determined using the method of MOORE and REYNOLDS (1997) and the computer program NEWMOD™ (REYNOLDS, 1985). The alternation and the d-spacing position of I/S basal reflections after glycolation were used to determine the different ordering types and the percentage of illite in I/S (MOORE and REYNOLDS, 1997). A reflection near 5 °2θ indicates random interstratification (Reichweite R = 0), one near 6.5 °2θ indicates R1 ordering and one between 7 and 8 °2θ long-range ordering (R > 1, MOORE and REYNOLDS, 1997).

VITRINITE REFLECTANCE

Coal rank was determined on 28 samples by measuring the reflectivity of vitrodetrinite (coalification expressed as vitrinite reflectance % R_{max}). Coal rank and Kübler index were measured on the same specimen. For vitrinite reflectance measurements, shales were cut perpendicular to sedimentary bedding or, if recognizable, to the cleavage and then embedded in resin. After polishing, the coal rank was determined by reflectivity

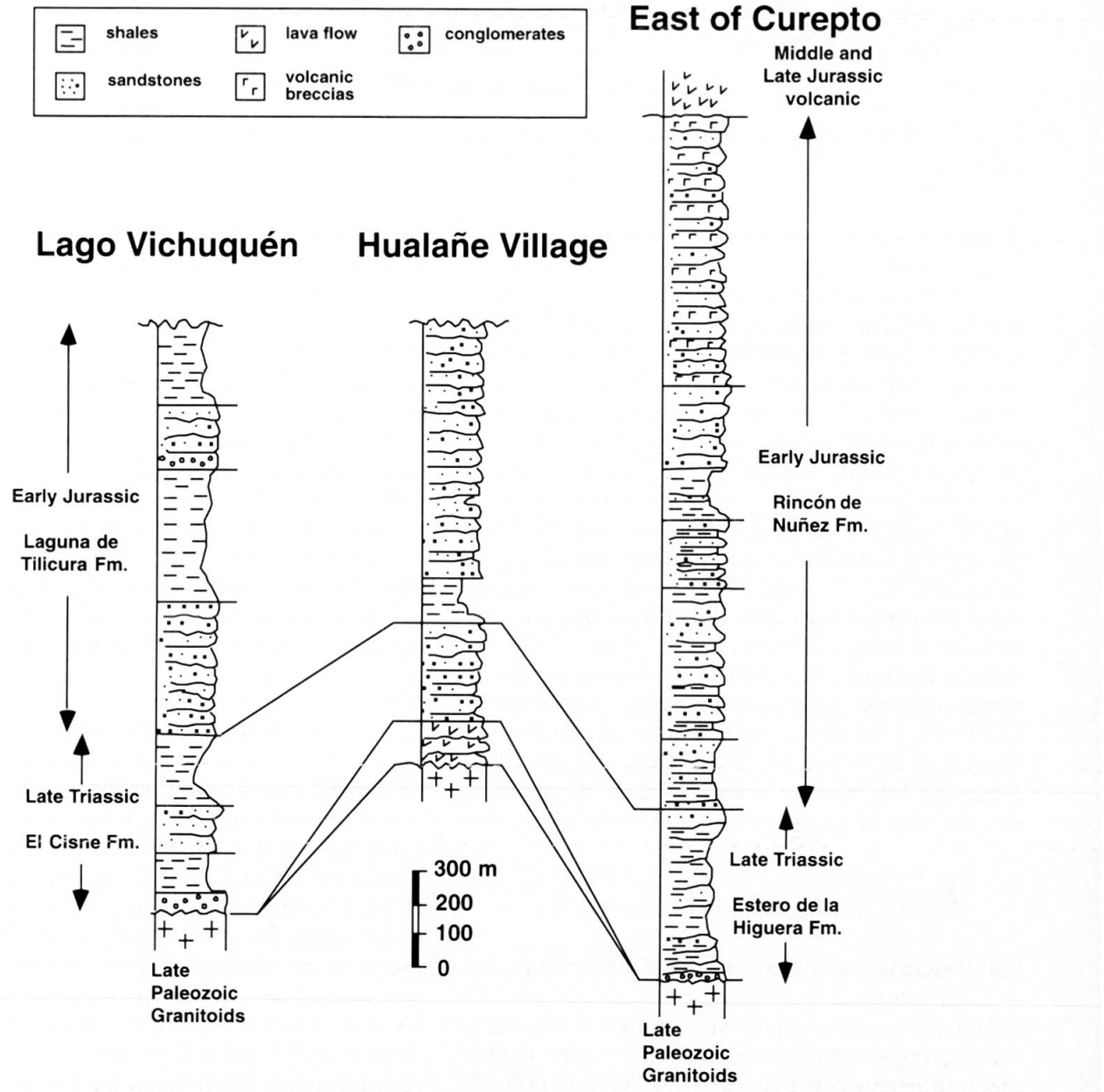

Fig. 3 Stratigraphic columns and estimated thickness of the Triassic–Jurassic in the Lago Vichuquén-Tilicura and Hualañé-Gualleco basins (after CORVALÁN, 1996).

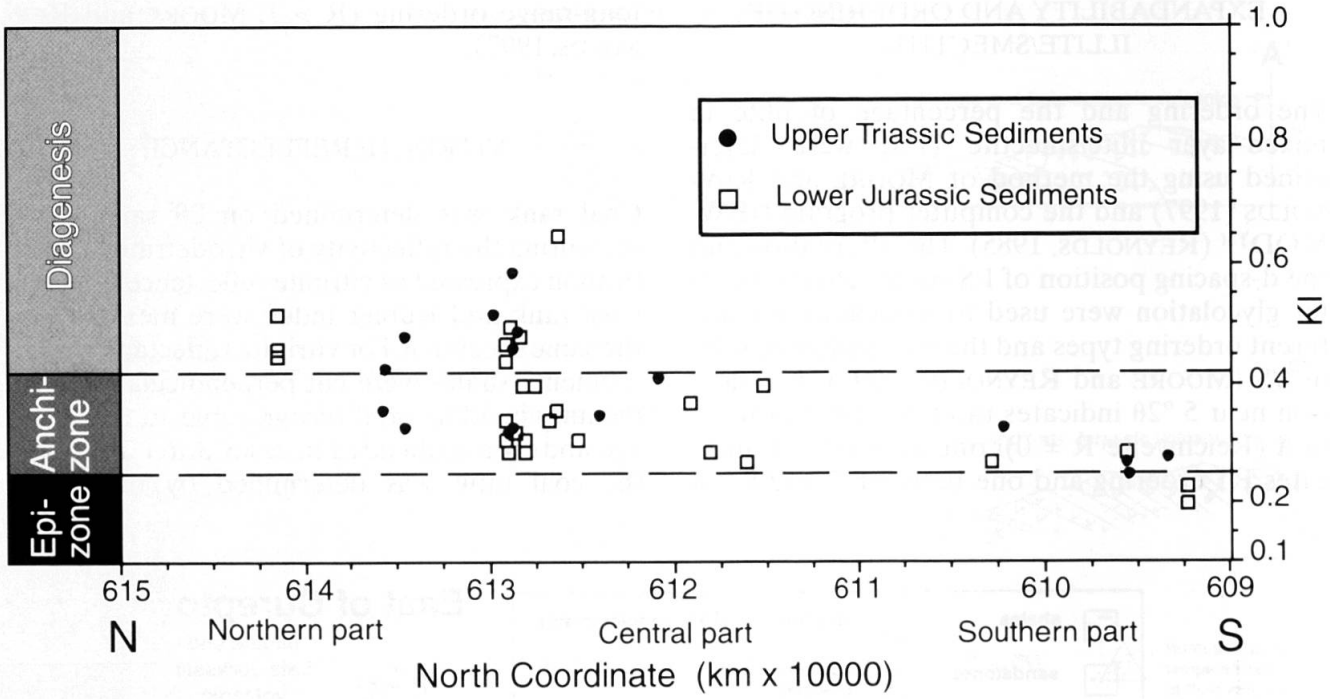

Fig. 4 Kübler index values plotted vs. UTM coordinates in N–S direction showing a decrease of KI from north to south.

measurements in oil immersion using a MPV-Leitz Orthoplan-photometer microscope with an 125× objective and an ocular with a magnification of 10×, monochromatic polarized light (546 nm) and a photomultiplier with a measurement area aperture of 2.5 μm^2. The arithmetic % R_{max}, % R_{min} and % R_R (mean maximum, mean minimum and random vitrinite reflectance; MACKOWSKY, 1982) were determined. Whenever possible, a minimum of 20 measurements from vitrodetrinite clasts was obtained for each sample. Synthetic garnet, zirconia and diamond, with reflectances of 1.72, 3.11 and 5.24%, were used as standards. The rank is based on the classification of coalification stages in STACH et al. (1982). The vitrinite reflectance is sensitive to changes in metamorphic grade mainly in the range from 0.25 to 8.0 % R_{max} or up to high epizonal conditions (STACH et al., 1982; FERREIRO MÄHLMANN, 1995; KOCH, 1997). Further details of data discrimination are given in FERREIRO MÄHLMANN (2001).

FLUID INCLUSION MEASUREMENTS

Fluid inclusions in fissure quartz were analyzed by microthermometry using a Leitz Laborlux 12 Pol microscope equipped with a Chaixmeca freezing-heating stage that is designed to work within the temperature range of –180 °C to +600 °C (POTY et al., 1976). Calibration was performed using the triple points of n-hexane (–94.3 °C), carbon dioxide (–56.6 °C), distilled water (0.0 °C), and the melting temperatures of appropriate chemical compounds supplied by the Merck Corporation. The uncertainty of measurements is on the order of ±0.1 °C within the range of –60 to +40 °C and ±1 °C outside this range. The detailed methodology for determining fluid inclusion bulk density, composition and temperature and pressure of fluid inclusion determination is described in MULLIS (1987).

Solid phases in quartz as well as within aqueous fluid inclusions were identified with the Scanning Electron Microscope (SEM) and chemical compositions were qualitatively determined using energy dispersive spectrometry (EDS).

MICROPROBE ANALYSES

Chemical analyses and scanning electron microscope (SEM) images of minerals were obtained using the JEOL JXA-8600 superprobe at the University of Basel. Olivine (Mg, Fe, Si), orthoclase (K,Al), synthetic graftonite (Mn), albite (Na) and wollastonite (Ca) were used as standards. All elements were measured using wavelength dispersive spectrometry, an accelerating voltage of 15 kV and a beam current of 10 nA. The detection limit was determined by measuring the just-detectable peak, corresponding to 3σ of the background count. In general, counting times for major and minor elements was 10 s and 20 s, respec-

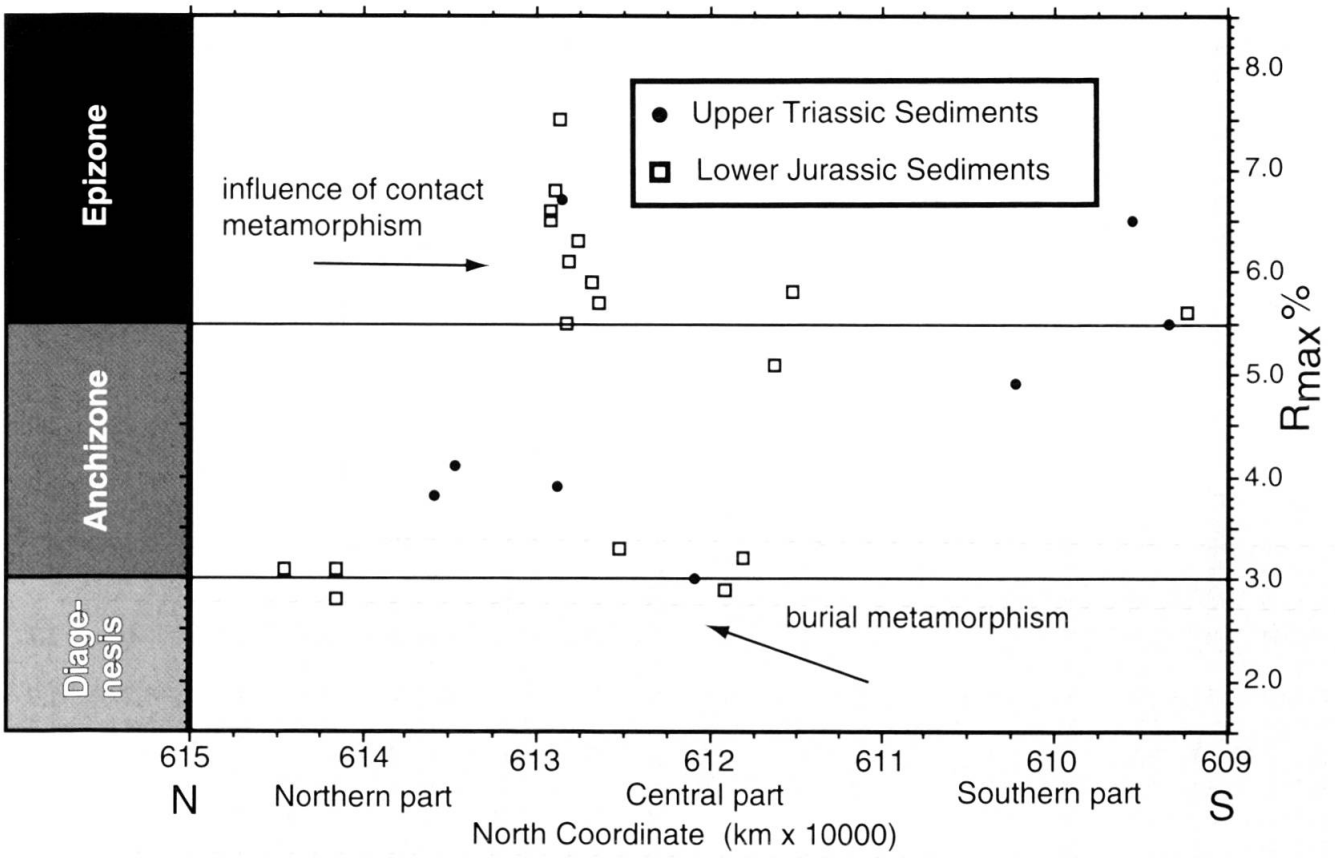

Fig. 5 Vitrinite reflection data plotted vs. UTM coordinates in N–S direction showing the probable influence of contact metamorphism and of burial metamorphism.

tivly and the background counting time was set to 4 s. The beam was focused to a spot size of 2 µm. Data were reduced using the PROZA correction program for all silicates, data of pumpellyite and epidote using the programm ZAF due to the high Fe-content. Microprobe analyses of chlorite were normalized to 28 oxygens and fulfill the criterion (Na+Ca+K) < 0.20 as a constraint for microprobe analyses uncontaminated by other phases (SCHMIDT et al., 1997).

Results

A total of 71 samples were analyzed including shales and slates, but also some sandstones and a few volcanic rocks. Incipient metamorphism in the study area is documented by the occurrence of several index minerals, various properties of illite and mixed-layer illite/smectite, vitrinite reflectance and fluid inclusion data. Results from Kübler index are presented first because they serve as a reference frame for other indicators of incipient metamorphism and are conventionally used to differentiate diagenesis, anchizone and epizone (KISCH, 1987).

KÜBLER INDEX

Kübler index was determined on 49 samples. KI values range from 0.18 to 0.65 $\Delta°2\theta$ (Table 1) and their regional distribution is depicted in Figs. 1, 2 and 4. In the Vichuquén-Tilicura basin, KI values of the high diagenetic zone (Jurassic sediments) are more frequent than KI values of the low anchizone (Triassic sediments). In the Hualañé-Gualleco basin, most KI values indicate anchi- and epizone, but no systematic difference in KI values between the Late Triassic and Early Jurassic sediments is observed. In general, KI values decrease southward but there is considerable scatter in the values (Fig. 4). In the south, NE of Curepto, the KI values belong to the low and high anchizone, whereas near Gualleco, most KI values are indicative of the high anchizone and epizone, respectively.

VITRINITE REFLECTANCE

Dispersed organic matter shows a broad range of coalification from 2.8 to 7.5% R_{max} (Table 1). The regional distribution of R_{max} data is depicted in Figs. 1–2 and plotted in a north-to-south section in

Table 1 Mineral assemblages, Kübler index and coal rank data. RF—Rock Formation. Vichuquén-Tilicura basin: 1—El Cisne Fm, 2—Laguna Tilicura Fm. Hualañé-Gualleco basin: 3—Estero de la Higuera Fm, 4—Rincón de Nuñez Fm. UT—Upper Triassic; LJ—Lower Jurassic. Abundance of minerals: X—abundant, O—low abundance, ?—presence questionable. *b* cell = K-white mica *b* cell dimension. Il/Sm—illite/smectite; Chl/Sm—chorite/smectite; Pg—paragonite and/or K-mica; Prl—pyrophyllite; Qtz—quartz; OM—organic material.

Sample	RF	Age	Il	Il/Sm	Chl	Chl/Sm	Prl	Pg	Qtz	OM	Kübler index Δ°2Θ	FWHM glycol Δ°2Θ	*b* cell (Å)	Rmax (%)	σ(Rmax)	Rmin (%)
H3-09	1	UT	O	O		O		O	O		0.43	0.42				
H3-10	1	UT	O	X		O			X	X	0.36	0.32	8.999	3.8	0.23	2.4
H3-07	1	UT	X	X					O		0.48	0.39				
H3-08	1	UT	O	O		O			O	X	0.33	0.29	8.996	4.1	0.21	2.5
H1-12	2	LJ	X	X	O				O	X	0.46	0.42		2.8	0.22	2.0
H1-01	3	UT	X	O				O	O	O	0.59	0.56				
H1-02	3	UT	X	?			X	O	O	X	0.33	0.84		3.9	0.24	2.2
H1-03	3	UT	X	?			X	O	O	O	0.46	0.56				
H1-04	3	UT	O	?					X	O	0.49	0.39		6.7	0.21	4.3
H2-08	3	UT	O	O	O		O		O		0.32	0.77				
H2-07	3	UT	X	O					O		0.52	0.43				
H4-04	3	UT	X						X	O	0.25	0.25	9.001	6.5	0.62	2.7
H4-06	3	UT	X						X		0.27	0.24	9.002			
H4-07	3	UT	X	?		O			X	O	0.33	0.3	9.000	4.9	0.27	1.9
H5-04	3	UT	X			O			O	X	0.28	0.25	9.007	5.5	0.47	1.4
H6-19	3	UT	X	O				O	X	O	0.41	0.37		3	0.25	1.4
H7-01	3	UT	O	O		?			X		0.35	0.33	9.002			
H7-02	4	LJ	X	?		O			X	X	0.31	0.27	9.000	3.3	0.31	2.1
H7-04	4	LJ	X						X	X	0.36	0.33	9.002	5.7	0.3	3
H7-05	4	LJ	O		O	?			X	X	0.29	0.24	9.000	6.8	0.44	3.1
H2-02	4	LJ	X						X		0.31	0.30	8.991			
H2-03	4	LJ	X	O		O		O	X	X	0.50	0.47		6.8	0.46	3.6
H1-07	4	LJ	X		?				X	X	0.44	0.38	8.986	6.6	0.38	3.5
H1-08	4	LJ	X			O			O	O	0.34	0.27	9.003			
H1-06	4	LJ	X		?				O	X	0.47	0.40		6.5	0.30	3.6
H2-05	4	LJ	X							X	0.32	0.33	9.001	7.5	0.48	4.0
H2-06	4	LJ	X	O					O		0.48	0.44				
H3-01	4	LJ	X						X	X	0.40	0.36	8.997	5.5	0.35	3.2
H3-02	4	LJ	X						X	O	0.31	0.30	8.998			
H3-03	4	LJ	X						X	X	0.29	0.30	8.992	6.1	0.25	4.0
H3-04	4	LJ	X						X		0.29	0.28	9.001			
H3-06	4	LJ	O	X					O	X	0.40	0.38	9.005	6.3	0.40	3.4
H4-05	4	LJ	X						X		0.29	0.27	8.997			
H4-08	4	LJ	O						X		0.27	0.23	9.004			
H1-05	4	LJ	O		O	?			X	X	0.34	0.29	9.008	5.9	0.32	3.4
H7-03	4	LJ	X	O					O	X	0.65	0.49				
H7-04	4	LJ	X						X	X	0.36	0.33	9.002	5.7	0.30	3.0
H7-02	4	LJ	X	?		O			X	X	0.31	0.27	9.000	3.3	0.31	2.1
H6-18	4	LJ	X						O	X	0.39	0.32	9.000	2.9	0.15	1.6
H6-17	4	LJ	O			O			X	O	0.39	0.37	8.999	3.2	0.29	2.3
H6-14	4	LJ	X	X					O	X				5.1	0.29	2.5
H6-15	4	LJ	O		O				X	X	0.27	0.27	9.005			
H6-13	4	LJ	X						X	X	0.40	0.33	8.995	5.8	0.25	3.2
H4-08	4	LJ	O						X		0.27	0.23	9.004			
H4-05	4	LJ	X						X		0.29	0.27	8.997			
H4-01	4	LJ	X		?				O		0.20	0.18	8.995			
H4-02	4	LJ	X		X			O	X		0.23	0.23		5.6	0.73	1.9

Fig. 5. The R_{max} values vary in a similar manner to the KI data and generally increase southward with considerable scatter in the data. The highest coal rank of the meta-anthracite stage is found in the vicinity of granodioritic-dioritic intrusions (Figs. 1–2).

In the northern part of the Vichuquén-Tilicura basin, the coal rank ranges from 2.8 to 3.1 % R_{max}

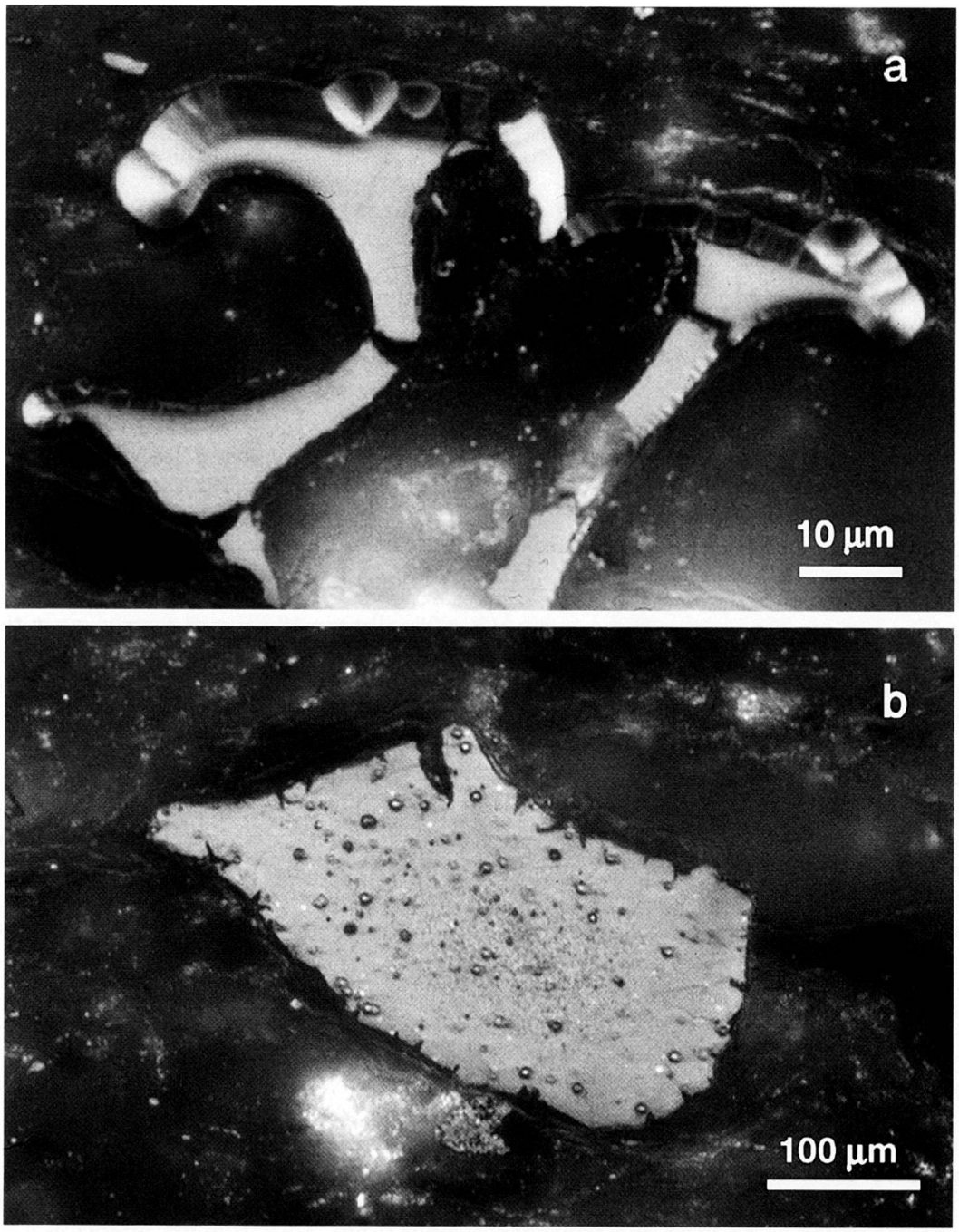

Fig. 6 (a) Texture of pyrolitic carbon in organic matter of sample H2-5. (b)Texture of natural coke in organic matter of sample H4-4.

(low anthracite stage or equivalent to the high diagenetic zone as determined by KI values), while in the southern part of this basin two values of 3.8 and 4.1 % R_{max} are found (transition of the anthracite to meta-anthracite stage or equivalent to the lower anchizone). In the northwestern part of the Hualañé-Gualleco basin, values vary between 2.9 and 3.3 % R_{max} (low anchizone) but north of the Río Mataquito, coal rank values increase from west to east. Samples with values >6 % R_{max} show textures of natural coke and pyrolitic carbon (Fig. 6) formed after chemical cracking of volatiles. The pyrolitic carbon forms spherical fibrolitic bodies (<50 µm) with helicitic extinction (anisotropic fibroblastic structure showing Brewster cross) and shows other typical optical features of a short and fast thermal overprint, as described by FERREIRO MÄHLMANN (2001). East of Curepto, the coal rank ranges from 4.9 to 6.5% R_{max} (meta-anthracite to semi-graphite stage or the low anchizone to epizone). As in the northwestern part of the Hualañé-Gualleco basin, the sample with the highest coal rank (R_{max} = 6.5%) also shows textures of pyrolitic carbon.

Table 2 Microthermometric results. (1) Host mineral. PQ—prismatic quartz, VQ—vein quartz. (2) Fluid inclusion population. (3) Inclusion type. psII—pseudosecondary fluid inclusion, II—secondary fluid inclusions. (4) Number of studied fluid inclusions. (5) VoT—volatile type. (6) V%—volume-% of the volatile part at room temperature. (7) Tm_{ice}—melting temperature of ice (°C). First number: mean value, second and third number: extreme values. (8) Tdcl—dissociation temperature of clathrate. (9) ThVol—homogenization temperature of the volatile part (°C), L—homogenization temperature to the liquid phase. (10) TH_2O-vol—homogenization temperature of the aqueous part with the volatile part (gas bubble), L—homogenization to the liquid phase. (11)-(13)—approximate mol% of H_2O, NaCl-equiv and CH_4-equiv. HHC— more than 1 mol% of hydrocarbons heavier than CH_4, A—anisotropic minerals—calcite, phyllosilicates, quartz.

Sample	1	2	3	4	5	6	7	8	9	10	11	12	13	14
					VoT	V%	Tm_{ice}	Tdcl	ThVol	TH_2O-vol				
H2	PQ	1	psII	19	CH_4	6	–6.1/–7.0; –5.2	12	no	187/167; 195 L	>95.5	3.1	<1	A
H2	PQ	2	II	26	CH_4	8	–4.5/–4.8; 4.2	12	no	223/213; 235 L	>96.7	2.3	<1	A
H6-18b	VQ	1	II	20	H_2O	5–6	n.m.		no	170–240 L	H_2O	NaCl	vol?	A
H6-18b	VQ	2	II	6	HHC	90	n.m.		–60/–63; –54 L	no			HHC	
H6-18b	VQ	3	II	5	CH_4	5	–3.6/–3.6; –3.5	13	no	179/175; 181 L	>97.1	1.9	<1	A
H6-18b	VQ	4	II	36	CH_4	6	–3.2/–3.3; –3.0	13	no	190/180; 199 L	>97.3	1.7	<1	A

DISTRIBUTION OF INDEX MINERALS

The main minerals identified by XRD are white mica (illite-muscovite) and quartz. Only a few samples contain chlorite, paragonite, K-mica, pyrophyllite, mixed-layer clay minerals (illite/smectite and chlorite/smectite) and albite. Mineral assemblages are listed in Table 1.

Pyrophyllite occurs in three closely spaced outcrops of Late Triassic grey shales (Estero de la Higuera Fm, Fig. 3) northwest of Hualañé (Fig. 1, Table 1). Kübler index values for two samples indicate low anchizone (KI $\Delta°2\theta$ = 0.32 and 0.33) and two samples (KI = 0.46 and 0.59) may be slightly affected by weathering.

Paragonite was identified in three samples with KI values of 0.50, 0.43 and 0.23 which are diagnostic of the high diagenetic zone and epizone, respectively. The first value is probably also influenced by weathering.

Biotite occurs in one sample (sample H5-03) located close to a diorite body in the southern part of the study area. The mineral assemblage is ferrosilite ($XFe_{0.6}$)-grunerite-actinolite/ magnesiohornblende-biotite-allanite (epidote) with plagioclase, stilpnomelane, ilmenite, titanite and apatite.

EXPANDABILITY AND ORDERING OF ILLITE/SMECTITE

Mixed-layer illite/smectite (I/S) is present in all samples from the Vichuquén-Tilicura basin and is characteristic of the high diagenetic and the low anchizone, but occurs only sporadically in anchizonal and epizonal samples from the southern Hualañé-Gualleco basin. Three types of mixed layering were observed: Type 1 is defined by the presence of the I/S ordering type R = 1 with 65 to 80% illite in I/S. Type 1 is present in the northern part of the Vichuquén-Tilicura basin (samples H1-10 to H1-12, H3-12 & H3-13) where KI values indicate high diagenetic conditions and R_{max} reaches approximately 3%. Type 2 is defined by the presence of the I/S ordering type, R = 3, with >90% illite in I/S. This type is present in the southern part of the Vichuquén-Tilicura Basin (samples H3-7 to H3-10) and in one sample (H3-6) from near Hualañé where KI values indicate high diagenetic to low anchizonal conditions and R_{max} reaches about 4%. Type 3 contains 85–90% illite in I/S and is designated as ordering type R > 1. It was found only in one sample in the Hualañé-Gualleco basin, east of Curepto.

THE K-WHITE MICA *b* CELL DIMENSION

The K-white mica *b* cell dimension ranges between 8.991–9.008 Å for 15 illites from the low anchizone, for 10 high anchizonal illites from 8.992–9.007 Å, and for a single epizonal illite a value of 8.995 Å was obtained. This leads to a mean K-white mica *b* cell dimension of 9.000 Å (σ=0.004; n=26). The cumulative frequency plot indicates that low pressure conditions prevailed (Fig. 7). A comparison of this data with that of GUIDOTTI and SASSI (1986) indicate a baric type similar to that of New Hampshire (x=9.003 Å; σ=0.004; n=40) implying low-pressure conditions.

FLUID INCLUSION MEASUREMENTS

Fluid inclusion populations were examined in two samples of fissure quartz taken from an Early Jurassic sedimentary formation in the Hualañé-

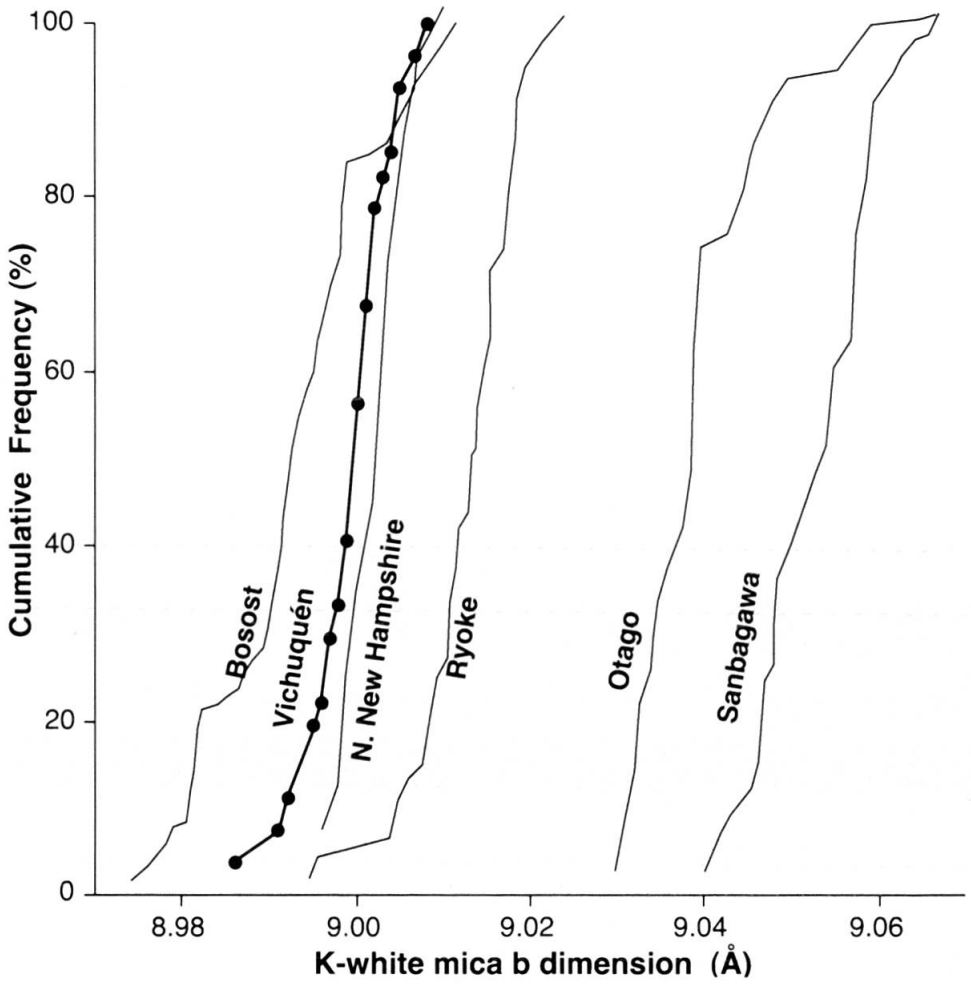

Fig. 7 Cumulative frequency data of values of the K-white mica *b* cell dimension for 25 anchizonal and one epizonal samples for Vichuquén. Reference curves are from SASSI and SCOLARI (1974) and SASSI (personal comm., 1999).

Gualleco basin (for location see Fig. 1). One sample is from the immediate proximity of a Middle Jurassic dioritic intrusion in the eastern Hualañé-Gualleco basin (sample H2-1) and the other sample originates from the bottom of the Early Jurassic sedimentary sequence, located near the contact with the Triassic sedimentary rocks (sample H6-18).

Two fluid inclusion populations were found in the northeastern locality: the older population consists of pseudosecondary inclusions, whereas the younger populaton is composed of secondary inclusions. Both inclusion populations contain an aqueous solution (Table 2) with a small amount of dissolved methane (<1 mol%) whose presence is evidenced by the occurrence of methane clathrate which dissociates (Td_{Cl}) at 12 °C. The melting temperature of ice (Tm_{Ice}) was converted to 3.1 mol% $NaCl_{eq}$ for population 1 and 2.3 mol% $NaCl_{eq}$ for population 2 based on experimental data of POTTER et al. (1978). These values are slightly too high, as the presence of clathrates lowers the salinity. The measured homogenization temperatures ($Th_{H2O\text{-}Vol}$) of 187 ± 20 °C for fluid population 1 and 223 ± 12 °C for fluid population 2 are, in the presence of some dissolved methane, interpreted as the minimum to approximate trapping temperatures. A minimum to approximate pressure of >1.3 kbar was calculated for population 1, based on the H_2O–CH_4–NaCl system of DUAN et al. (1992). No pressure estimate is possible for population 2 due to the limitations of the fluid system concerned (DUAN et al., 1992).

Four fluid inclusion populations are observed from the bottom of the Early Jurassic sedimentary sequence. Fluid inclusion population 1 formed during or immediately following the precipitation of quartz. Fluid inclusions are obscured by a lot of comtemporaneously included solids such as phyllosilicates and calcite (Fig. 8). This fluid inclusion population is interpreted to have formed from a fluid containing substantial amounts of Si, Al, Ca, Na, K and CO_2 during diagenetic conditions.

Fluid inclusions of population 2 were detected within a quartz rim overgrowing early quartz.

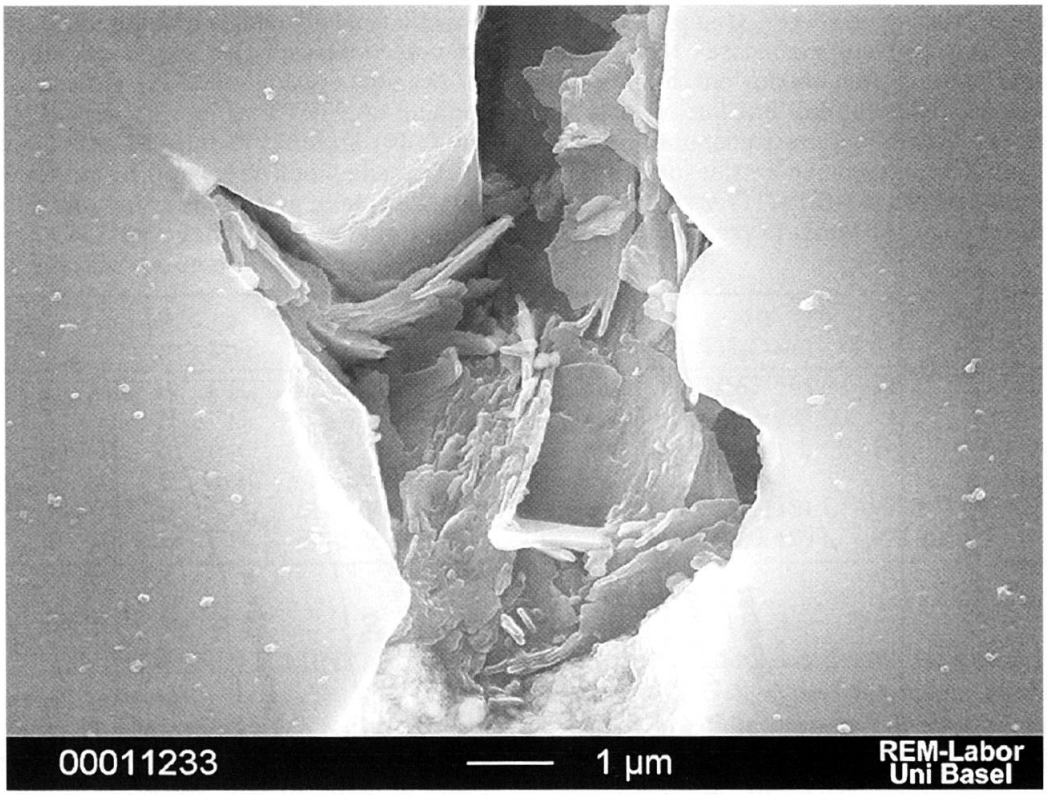

Fig. 8 SEM photograph showing phyllosilicate inclusions in cavities of a quartz crystal.

They are up to >90 vol% a mixture of hydrocarbons and homogenize at –60 ±4 °C. No solid CO_2 was observed at low temperatures indicating a fluid composition of 80 to 90 mol% methane and 10–20 mol% higher hydrocarbons (MULLIS, 1979).

Inclusion populations 3 and 4 frequently occur within the overgrown quartz rim and postdate population 2. These inclusions contain a methane bearing aqueous solution (<1 mol% CH_4) derived from clathrate that dissociates (Td_{Cl}) at 13 °C. Salinities of 1.9 mol% $NaCl_{eq}$ were determined for population 3 and 1.7 mol% $NaCl_{eq}$ for population 4, using the freezing point depression of aqueous sodium solutions (Tm_{Ice}) of POTTER et al. (1978). Due to the presence of clathrates salinities are slightly overestimated. Bulk homogenization temperature ($Th_{H2O\text{-}Vol}$) for population 3 and 4 are 179 ± 4 °C and 190 ± 10 °C, respectively (Table 2). The aqueous solutions were enriched with methane during inclusion formation and hence these temperatures are interpreted as minimum to approximate trapping temperatures. Referring to the P–V–T data of the H_2O–CH_4–NaCl system (DUAN et al., 1992), minimum to approximate formation pressures of fluid inclusion population 3 and 4 are 1.4 and 1.3 kbar , respectively.

METAMORPHIC MINERALS AND MINERAL CHEMISTRY IN VOLCANIC ROCKS

In addition to shales and slates, a few lavas and volcaniclastic rocks were studied. In the upper part of the Early Jurassic formation southeast of the Río Mataquito the sedimentary rocks are increasingly interbedded with lavas and andesitic breccias (MOREL, 1981). Lava flows of Late Jurassic age are exposed in the most northeastern part of the Hualañé-Gualleco basin. They contain euhedral phenocrysts of plagioclase, K-feldspar and augite. Chlorite and calcite are the main alteration products. Plagioclase is partly to completely albitized. Newly formed albite shows a compositional range between $An_{0.4}$ and An_{21} although a majority lies in the range of $An_{0.4}$ and An_8.

Epidote occurs frequently in the lava flows together with chlorite, titanite, magnetite, calcite and locally pumpellyite and grandite. It replaces plagioclase and clinopyroxene phenocrysts along fissures, is observed in minor amounts in small crystals in the groundmass and preferentially fills the cores of vugs and interstices. Two types of epidote are distinguished in the southern part: (1) a dusty, brownish variety with a pistacite component of 14.9 to 27.6 and (2) a light-yellow variety

that always occurs inside the brownish one and has a pistacite component between 30.6–42.7. In the eastern central part three types can be distinguished. Type 1 has a brownish color and shows a pistacite component between 28 and 33. Type 2 is of yellow color and is characterized by a pistacite component of 39 to 43. The presence of Ce, Nd and La suggests allanitic compositions in the center of type 3 grains.

Titanite occurs as dusty granules or small spherical aggregates at the rim of vugs and interstices associated with chlorite, epidote and as dispersed spots in the groundmass. Titanite in the study area has Al_2O_3 contents between 2.7–4.8 wt% and Fe_2O_3 contents between 1.4–5.9 wt%, similar to prehnite-pumpellyite facies terranes in central Sweden (NYSTRÖM, 1983) and the metaandesites of the Celica Formation in southwestern Ecuador (AGUIRRE, 1992). There is no increase in titanium content with metamorphic grade as seen in the Taveyanne formation of western Switzerland (SCHMIDT et al., 1997).

Chlorite is the most common metamorphic mineral in the Middle to Late Jurassic volcanic and volcanoclastic rocks. It frequently occurs as replacement patches inside plagioclase and clinopyroxene phenocrysts, as inclusions in vugs and also as interstitial material in the groundmass. Most occurrences are pale-green, although yellowish-green pleochroitic types appear with anomalously deep blue to brownish grey interference colours. The low $\Sigma(Na+K+Ca)$ contents (>0.2), based on a calculated sum of 28 oxygen atoms indicate very low contents of interlayered smectite.

A rock specimen containing pumpellyite from the most northeastern part of the Hualañé-Gualleco basin, with the assemblage grandite-epidote-chlorite-titanite-calcite-magnetite-allanite, is reported for the first time from this area. Although optically homogenous, two intergrown pumpellyite types can be distinguished chemically. Pumpellyite of type 1 has FeO* contents between 9.25 and 11.75 wt% and Al_2O_3 contents between 19.69 and 21.64 wt%. Pumpellyite of type 2 has lower FeO* values ranging between 5.56–8.8 wt%, although the Al_2O_3 values are greater than type 1 and range between 21.24 to 23.03 wt%.

Grandite was observed in the same thin section as pumpellyite and allanite and ocurs as framboidal grains with a diameter of up to 20 µm within chlorite patches of the groundmass and also in chlorite-epidote vugs. XFe^{3+} values range from 53.3 to 62.7% and small amounts of Mg are present (max. 0.36 wt%). Grandite analyses have low totals (between 95 and 99 wt%), a feature shared by framboidal grandites elsewhere and attributed by COOMBS et al. (1977) to fluid-filled

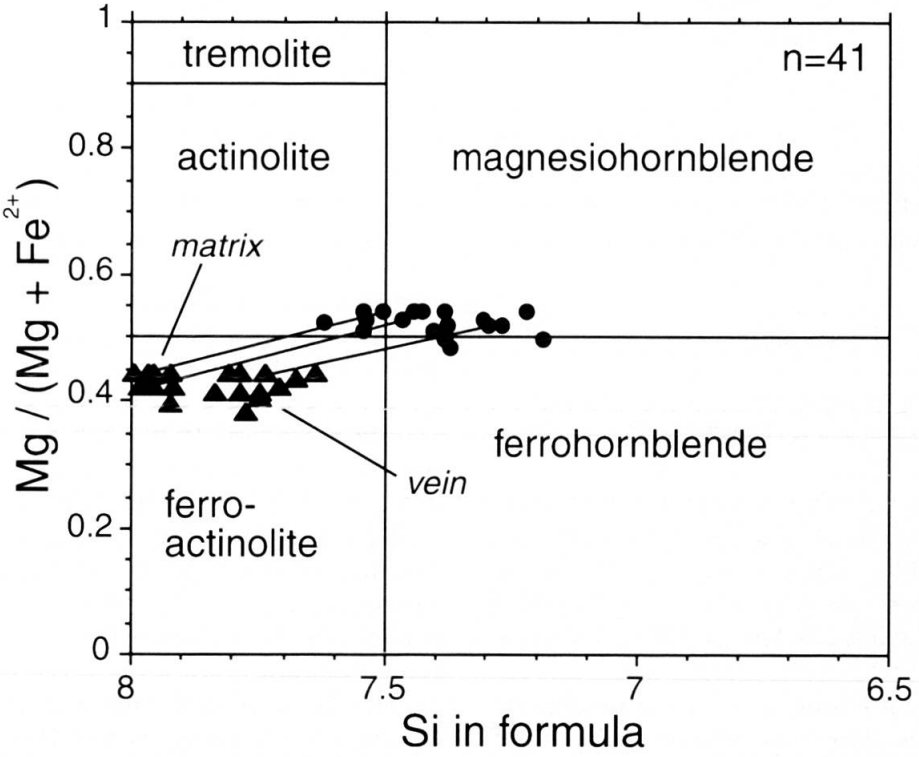

Fig. 9 Compositional field of amphiboles that result from contact metamorphism (LEAKE et al., 1997). Lines indicate intergrown phases; circle: high temperature contact metamorphic event, triangle: retrograde contact metamorphic event

microcavities. The grandite-pumpellyite-chlorite-epidote assemblage may form during the burial induced metamorphism of basic volcanic rocks, as described by COOMBS et al. (1977) from southern New Zealand, metamorphosed to prehnite-pumpellyite facies, or from upper zeolite facies rocks as reported by AGUIRRE (1992) in SW Ecuador. COOMBS et al. (1977) state that grandite-chlorite assemblages are common in metabasites of very low metamorphic grade, but are eliminated before the onset of greenschist facies conditions because grandite is incompatible with chlorite in the presence of quartz under such conditions.

MINERAL CHEMISTRY IN PELITIC ROCKS

Contact metamorphic field relationships between Jurassic intrusions and Jurassic sedimentary rocks are only visible in fresh roadcuts. A hornfels (H5-03) with quartz, plagioclase, flakes of biotite with inclusions of Ti-Fe-phases and anhedral ferrosilite ($XFe_{0.6}$) was taken a few meters away from an intrusion near the Gualleco valley. A vein in the specimen contains euhedral ferrosilite ($XFe_{0.6}$) and actinolite-magnesiohornblende which are partly replaced along rims by ferroactinolite, as well as biotite, chlorite and stilpnomelane which represent the mineral assemblage of the retrograde part of the contact metamorphic event. The vein also contains euhedral allanite and apatite. The chemical compositions of actinolite-magnesiohornblende and ferroactinolite of the matrix and the vein are shown in Fig. 9 (after LEAKE, 1997). Ferroactinolite occurs also in the rock matrix adjacent to the vein. The matrix ferroactinolite has a higher Si content than the ferroactinolite in the vein, although the $Mg/(Mg+Fe^{2+})$ ratios are similar for both matrix and vein ferroactinolite.

Discussion

COMPARISON BETWEEN COAL RANK, KI AND MINERAL ASSEMBLAGES

Data from a large number of regional metamorphic terrains show that a general relationship exists between Kübler index and coal rank: as the Kübler index decreases, the vitrinite reflectivity increases (for a review see KISCH, 1987). The maturation of organic matter is known to be an irreversible process and coal rank in the diagenetic and the anchizone has been shown to be more sensitive than KI to an increase in temperature (WOLF, 1975). Kübler index and coalification increase simultaneously up to anchizonal conditions in the study area (Fig. 10). The black line in Fig. 10 represents the vitrinite reflectance-Kübler index correlation found as a mean for different tectono-metamorphic histories (FERREIRO MÄHLMANN, 1995) and for orogenic low-temperature-low-pressure events under long-time heating conditions close to peak temperatures (FERREIRO MÄHLMANN, 2001). The high diagenetic to anchizonal values of the Vichuquén-Tilicura basin are close to that trend. This group of samples is therefore interpreted to represent the low-grade metamorphic burial event that reached up to anchizonal conditions. Certain samples violate this general trend, showing KI values of the anchizone but coal rank data of the epizone (Fig. 10). In addition, these samples show the textures with natural coke and pyrolitic carbon. These increased vitrinite reflectance values are interpreted as the result of a high temperature heating event of short duration caused by the emplacement of intrusions nearby. Further to the south, near Gualleco, KI values generally indicate epizonal conditions and corroborate with the coal rank data (Figs. 1 and 10). It is not clear whether this is the result of the proximate dioritic-granodioritic intrusions or if the KI values are a consequence of an increase in stratigraphic thickness, resulting also in a higher burial induced metamorphic grade.

Thermal maturity models, calibrated by vitrinite reflectance data, are very useful in determining the thermal histories during very low-grade metamorphism in sedimentary basins (e.g. ENGLAND and BUSTIN, 1985; LANGENBERG and KALKREUTH, 1991; GALLAGHER and SAMBRIDGE, 1992; SACHSENHOFER et al., 2000; FERREIRO MÄHLMANN, 2001). It is possible to model the burial metamorphic conditions of the Hualañé-Gualleco basin by using "Seditools" (PETSCHICK, 1996, based on LOPATIN, 1971 and WAPLES, 1980). The lowest vitrinite reflectance values (R = 2.9–3.2), a total thickness of 4600 m of Jurassic rocks (including 2100 m of eroded rocks, ESCOBAR, 1976; CORVALÁN, 1976) and a geothermal gradient of 35 °C as inferred from fluid inclusion data were assumed in the model. However, it was not possible to model high coal rank data (>5.0 R_{max}) with such a burial metamorphic model and the above parameters. Other parameters, such as locally occurring higher heat flow during contact metamorphism, could be responsible for this increase in coal rank data.

The KI and coal rank values are compared with phases identified using XRD that are characteristic for each metamorphic zone. Sedimentary rocks with illite/smectite are located in the high diagenetic zone. Paragonite is present from the

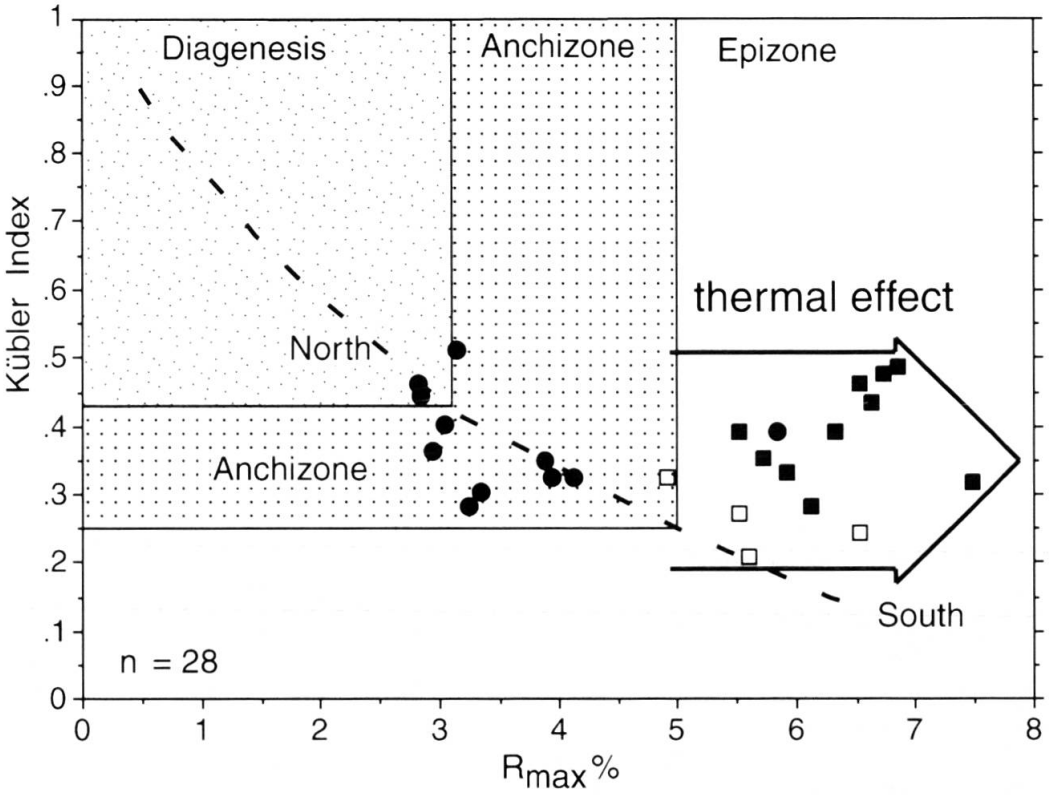

Fig. 10 Correlation of Kübler index versus coal rank data. Full dots—samples far away from granitic intrusions. Square—samples in the vicinity of intrusions or with organic material containing natural coke or pyrolitic carbon; open square—Gualleco intrusion; full square—Hualañé intrusion. The black line represents the vitrinite reflectance-Kübler index correlation found as a mean for different tectono-metamorphic histories (FERREIRO MÄHLMANN, 1995).

beginning of the anchizone to the lower epizone, and pyrophyllite appears in the lower anchizone. The mineral assemblage grandite-pumpellyite-chlorite-epidote of a Jurassic volcanic rock indicates higher zeolite to subgreenschist facies conditions which correlate with the observed KI and coal rank data.

TEMPERATURE AND PRESSURE DETERMINATION

"Chlorite thermometry" in very low-grade metamorphic rocks (CATHELINEAU, 1988) was recently reviewed by MERRIMAN and PEACOR (1999). Although its usefulness has been questioned (ESSENE and PEACOR, 1995; SHAU et al., 1990; JIANG et al., 1994; SCHMIDT et al., 1999), the "chlorite geothermometer" has been applied to four samples of this study. The andesite H7-6, located east of Hualañé, containing the assemblage chlorite-grandite-epidote-pumpellyite, yields a temperature of 237 ± 20 °C (n = 67). For two other volcanic rocks, located ESE of Curepto, containing no diagnostic assemblages, the chlorite temperatures are 253 ± 23 °C (n = 45) and 296 ± 25 °C (n = 60). The metapelite sample H4-2, located south of Gualleco and containing the assemblage chlorite-muscovite-paragonite-quartz, has a coal rank of 5.6 % R_{max} and a KI value of 0.23 Δ°2θ. It yields a temperature of 281 ± 16 °C (n = 8). The absolute temperature values are to be questioned but lie within the temperature range inferred from KI and coal rank. Chlorite formation within these samples is therefore considered to be part of the burial metamorphic history.

The measured minimum trapping temperatures of the various fluid inclusion populations in the two studied quartz veins show a similar temperature range. The KI values range between late diagenetic and low anchizonal values in nearby situated rocks, whereas all coal rank values indicate epizonal conditions and show evidence of contact metamorphism. Fluid inclusion populations are interpreted to have formed during the burial induced heating event. If a T ≥ 190 °C and p ≥ 1.3 kbar are assumed as well as $P_{fluid} = P_{total}$, an overburden of ca. 4.8 km can be deduced (rock density ≈ 2.7). The corresponding geothermal gradient is calculated to be >35 °C/km.

The KI, mineral paragenesis in pelitic and volcanic rocks, K-white mica *b* cell dimension and

"chlorite geothermometry" suggest a low-grade burial metamorphic history for the sediments of the Hualañé-Gualleco and the Vichuquén-Tilicura basins. The transformation of R1 to R3 observed in the southern part of the Vichuquén-Tilicura basin probably occured at a temperature of 170–180 °C (POLLASTRO, 1993). Smectite contents of 1–10% in the anchizone imply a burial depth of around 5 km at temperatures between 150 and 230 °C (see MERRIMAN and FREY, 1999).

The formation temperatures of the contact metamorphism in the immediate proximity of a hornfels with the assemblage ferrosilite ($XFe_{0.6}$)-ferroactinolite/magnesiohornblende-biotite were calculated based on coexisting plagioclase with An_{57} and magnesiohornblende with Al(VI) = 0.12, NaA = 0.94 and Si = 7.3 pfu using the amphibole-plagioclase thermometer of HOLLAND and BLUNDY (1994). Calculated temperatures of the edenite-tremolite solid solution lie within a range of 655 °C to 691 °C and a pressure of <4 kbar. Due to this increased temperatures, the sedimentary rocks near this sample show a strong increase in coal rank and KI values. HÉROUX and TASSÉ (1990) made similar observations in the Lower Ordovician Beckmantown Group in the St. Lawrence Lowlands in Quebec. Reflectance anomalies of organic matter are not only related to intrusions not exceeding a distance of 5 km, but also to major faults which they consider to be the pathways for hydrothermal fluids which transported the heat required to increase the reflectance of the organic matter.

The different methods used record different steps of the thermal evolution of the basin. KI, mineral assemblages, "chlorite geothermometry" and fluid inclusion thermometry reflect the various stages of the burial history, whereas the locally increased vitrinite reflectance and KI, as well as the hornfels paragenesis are the result of the thermal conditions either induced during intrusion of a magmatic body or by heat transfer from a hydrothermal fluid. All data point to a general thermal evolution under high heat flow condition and a low temperature-low pressure to high temperature-low pressure metamorphic history.

Acknowledgements

We would like to thank the Servicio Geológico de Chile for logistic support in the field, and Mario Vergara and Luis Aguirre, Universidad de Chile, for their help and information regarding the field area. We are very thankful to Prof. Karl Ramseyer, Universität Bern, for a critical review pointing out some weak parts of the paper as well to an anonymous reviewer. We thank Prof. Karl Seifert, University of Iowa, and Dr. George Morris, Département de Minéralogie in Geneva, for critically reading and correcting the last version. We also thank Jacques Metzger, Département de Minéralogie in Geneva for redrawing an earlier version of Fig. 1. Last but not least we thank Prof. Martin Engi, Universität Bern, for his careful editorial reviews. All authors wish to thank Martin Frey, the former head of the departement and leader of our group in Basel, who inspired and motivated us to achieve the best possible results. This study is part of the Ph.D. thesis of M.B. which was financially supported by the Swiss National Science Foundation Grants Nr. 20-43122.95, 20-50625.97 and 20-56842.99.

References

AGUIRRE, L. (1992): Metamorphic pattern of the Cretaceous Celica Formation, SW Ecuador, and its geodynamic implications. Tectonophysics 205, 223–237.

AGUIRRE, L., FERRAUD, G.G., MORATA, D., VERGARA, M. and ROBINSON, D. (1999): Time interval between volcanism and burial metamorphism and rate of basin subsidence in a Cretaceous Andean extension setting. Tectonophysics 313, 433–447.

AGUIRRE, L., LEVI, L. and OFFLER, R. (1978): Unconformities as mineralogical breaks in the burial metamorphism of the Andes. Contrib. Mineral. Petrol. 66, 361–366.

AGUIRRE, L., ROBINSON, D., BEVINS, R.E., FONSECA, E., VERGARA, M., CARRASCO, J. and MORATA, D. (1997): The Valle Nevado stratified sequence: chemistry and alteration pattern. Vol.2, 1195–1199. VIII Congreso Geológico de Chileno, Antofagasta, Chile.

CATHELINEAU, M. (1988): Cation site occupancy in chlorites and illites as a function of temperature. Clay Min. 23, 471–485.

COOMBS, D.S., KAWACHI, Y., HOUGHTON, B.F., HYDEN, G., PRINGLE, I.J. and WILLIAMS, J.G. (1977): Andradite and andradite-grossular solid solutions in very low-grade regionally metamorphosed rocks in southern New Zealand. Contrib. Mineral. Petrol. 63, 229–246.

CORVALÁN, J. (1976): El Triásico y Jurásico de Vichuquén-Tilicura y de Hualañé, provincia de Curicó. Implicaciones Paleogeográficas. In: Congr. Geol. Chileno, No. 1, A137– A154.

CORVALÁN, J. (1982): El Límite Triásico-Jurásico en la Cordillera de la Costa de las Provincias de Curicó y Talca. 3, F63–F85. III Congreso Geológico Chileno, Concepcion, Chile.

CORVALÁN, J. (1994): El Triásico y Jurásico de Vichuquén, Hualañé, Curepto y Gualleco. Unpublished map, Servicio Nacional de Geología y Minería.

DALLA TORRE, M. and FREY, M. (1997): The evolution from disordered Ad to ordered 2M1 white K-mica polytype in low-temperature metamorphosed sedimentary rocks. Schweiz. Mineral. Petrog. Mitt. 77, 149–159.

DUAN, Z., MØLLER, N., GREENBERG, J. and WEARE, J. (1992): The prediction of methane solubility in natural waters to high ionic strength from 0 to 250 °C and from 0 to 1600 bar. Geochim. Cosmochim. Acta, 56, 1451–1460.

ENGLAND, T.D. and BUSTIN, R.M. (1985): Effect of thrust faulting on organic maturation in the southeastern Canadian cordillera. Advances Org. Geochem. (eds: LEYTHÄUSER, D. and RULLKÖTTER, J.). Vol. 10, 609–616.

ESSENE, E.J. and PEACOR, D.R. (1995): Clay mineral thermometry – a critical perspective. Clay Clay Min. 43, 540–553.

FERREIRO MÄHLMANN, R. (1995): Das Diagenese-Metamorphose Muster von Vitrinitreflexion und Illit-

Kristallinität in Mittelbünden und im Oberhalbstein. Teil I. Bezüge zur Stockwerktektonik. Schweiz. Mineral. Petrog. Mitt. 76 (1), 23–46.

FERREIRO MÄHLMANN, R. (2001): Correlation of very low-grade data to calibrate a thermal maturity model in a nappe tectonic setting, a case study from the Alps. Tectonophysics 334, 1–33.

GALLAGHER, K. and SAMBRIDGE, M. (1992): Catagenesis of argillaceous sedimentary rocks. Geosci. Can. 4, 177–188.

GANA, P. and HERVÉ, F. (1983): Geología del Basamento Cristalino en la Cordillera de la Costa entre los ríos Mataquito y Maule, VII Región. Chile. Rev. Geol. Chile 19/20, 37–56.

GONZALES-BONORINO, F. (1970): Series metamórficas del basamento cristalino de la Cordillera de la Costa, Chile. Anales de la Facultad de Ciencias Físicas y Matemáticas, Departamento de Geología, Editorial Universitaria, Santiago, Chile, nr. 37, 68–82.

GUGGENHEIM, S., BAIN, D.C., BERGAYA, F., BRIGATTI, M.F., DRITS, V.A., EBERL, D.D., FORMOSO, M.L.L., GALÁN, E., MERRIMAN, R.J., PEACOR, D.R., STANJEK, H. and WATANABE, T. (2002): Report of the Association Internationale pour l'Étude des Argiles (AIPEA). Nomenclature commitee for 2001: Order, disorder and crystallinity in phyllosilicates and the use of the "crystallinity index". Clay Min. 37, 389–393.

GUIDOTTI, C.V. and SASSI, F.P. (1986): Classification and correlation of metamorphic facies series by means of muscovite b_0 data from low-grade metapelites. N. Jb. Mineral. Abh. 153, 363–380.

HÉROUX, Y. and TASSÉ, N. (1990): Organic-matter alteration in an early Paleozoic basin: Zonation around mineral showings compared to that around intrusions, St. Lawrence Lowlands, Quebec, Canada. Bull. Geol. Soc. Am. 102, 877–888.

HERVÉ, F., KAWASHITA, K. and MUNIZAGA, F. (1982): Edades Rb/Sr de los cinturones metamorficos pareados de Chile Central. Vol. 2, D116–D135. III Congreso Geológico Chileno.

HOLLAND, T. and BLUNDY, J. (1994): Non-ideal interactions in calcic amphiboles and their bearing on amphiboles-plagioclase thermometry. Contrib. Mineral. Petrol. 116, 433–447.

JIANG, W.T. and PEACOR, D.R. (1993): Formation and modification of metastable intermediate sodium potassium mica, paragonite and muscovite in hydrothermally altered metabasites from northern Wales. Am. Mineral. 78, 782–793.

JIANG, W.T., PEACOR, D.R. and BUSECK, P.R. (1994): Chlorite geothermometry? – Contamination and apparent octahedral vacancies. Clay Clay Min. 42, 593–605.

KISCH, H.J. (1987): Correlation between indicators of very-low-grade metamorphism. In: FREY, M. (ed.): Low Temperature Metamorphism, Blackie & Son, Glasgow, 227–300.

KISCH, H. (1991): Illite crystallinity: recommendations on sample preparation, X-ray diffraction setting, and interlaboratory samples. J. Metamorphic Geol. 9, 665–670.

KOCH, J. (1997): Upper limits for vitrinite and bituminite reflectance as coalification parameters. Int. J. Coal. Geol. 33, 169–173.

KÜBLER, B. (1967): La Crystallinité de l'illite et les zones tout à fait supérieures du métamorphisme. Étages tectoniques. Colloq. Neuchâtel, 105–122.

KÜBLER, B. (1984): Les indicateurs des transformations physiques et chimiques dans la diagenèse, température et calorimétrie. In: LAGACHE, M. (ed.): Thérmométrie et barométrie géologiques, Soc. Franç. Minér. Crist., Paris, 489–596.

LANGENBERG, W. and KALKREUTH, W. (1991): Tectonic controls on regional coalification and vitrinite-reflectance anisotropy of Lower Cretaceous coals in the Alberta foothills. Bull. Soc. géol. France 162/2, 375–383.

LEAKE, B., WOLLEY, A., ARPS, C., BIRCH, W., GILBERT, C. and GRICE, J. (1997): Nomenclature of Amphiboles: Report of the Subcommittee on amphiboles of the IMA. Can. Mineral. 35, 219–246.

LEVI, B. (1969): Burial metamorphism of a Cretaceous volcanic sequence west from Santiago, Chile. Contrib. Mineral. Petrol. 24, 30–49.

LEVI, B., AGUIRRE, B. and NYSTRÖM, J.O. (1982): Metamorphic gradients in burial metamorphosed vesicular lavas: comparison of basalt and spilite in Cretaceous basic flows from Central Chile. Contrib. Mineral. Petrol. 80, 49–58.

LOPATIN, N.V. (1971): Temperature and geologic time as factor in coalification (in Russian). Izv. Akad. Nauk. SSSR. Ser. Geol. 3, 95–106.

MACKOWSKY, M.T. (1982): Rank determination by measurement of reflectance on vitrinites. In: STACH, F., MACKOWSKY, M., TEICHMÜLLER, M., TAYLOR, G., CHANDRA, D. and TEICHMÜLLER, R. (eds): Textbook of Coal Petrology, Bornträger, Stuttgart, 319–329.

MERRIMAN, R.J and FREY, M. (1999): Patterns of very low-grade metamorphism in pelitic rocks. In: FREY, M. and ROBINSON, D. (eds): Low-grade metamorphism, Blackwell Science Ltd, 61–107.

MERRIMAN, R.J. and PEACOR, D.R. (1999): Very low-grade metapelites: mineralogy, microfabrics and measuring reaction progress. In: FREY, M. and ROBINSON, D. (eds): Low-grade metamorphism, Blackwell Science Ltd, 10–60.

MOORE, D.M. and REYNOLDS, R.C. (1997): X-Ray Diffraction and the Identification and Analysis of Clay Minerals. Oxford University Press, New York, 378 pp.

MOREL, R. (1981): Geología del sector norte de la hoja Gualleco, entre los 35°00' y los 35°10' latitud sur, provincia de Talca, VII Región, Chile. Tesis de Grado, M. Cs., Universidad de Chile, Departamento de Geología, Santiago.

MULLIS, J. (1979): The system methane-water as a geological thermometer and barometer from the external part of the Central Alps. Bull. Minér. 102, 526–536.

MULLIS, J. (1987): Fluid inclusion studies during very low-grade metamorphism. In: FREY, M. (ed.): Low Temperature Metamorphism, Blackie, Glasgow and London, 162–199.

MUNIZAGA, F., AGUIRRE, L. and HERVÉ, F. (1973): Rb/Sr ages of rocks from the Chilean metamorphic basement. Earth Planet. Sci. Lett. 18, 87–91.

NYSTRÖM, O.J. (1983): Pumpellyite-bearing rocks in central Sweden and extent of host rock alteration as a control of pumpellyite composition. Contrib. Mineral. Petrol. 83, 159–168.

NADEAU, P.H. and REYNOLDS, R.C. JR. (1981): Burial and contact metamorphism in the Mancos shale. Clay Clay Min. 29, 249–259.

PETSCHICK, R. (1996): ©Program SediTools. Version 1.1.2. Freeware. http://servermac.geologie.uni-frankfurt.de/Staff/Homepages/petschick/SediTools/SediTools.html.

POLLASTRO, R.M. (1993): Considerations and applications of the illite/smectite geothermometer in hydrocarbon-bearing rocks of Miocene to Mississippian age. Clay Clay Min. 41, 119–133.

POTTER, R., CLYNNE, M. and BROWN, D. (1978): Freezing point depression of aqueous sodium solutions. Econ. Geol. 73, 284–285.

POTY, B., LEROY, J. and LEON, J. (1976): Un nouvel appareil pour la mesure des températures sous le microscope: l'installation de microthermométrie Chaixmeca. Bull. Soc. géol. France 99, 182–186.

REYNOLDS, R.C. (1985): NEWMOD™, a computer program for the calculation of one-dimensional diffraction patterns of mixed-layer clays.

SACHSENHOFER, R.F., DUNKL, I., HASENHÜTTL, C. and JELEN, B. (1998): Miocene thermal history of the southwestern margin of the Styrian Basin: vitrinite reflectance and fission track data from the Pohorje/Kozjak area. Tectonophysics 297, 17–29.

SACHSENHOFER, R.F., KOGLER, A., POLESNY, H., STRAUSS, P. and WAGREICH, M. (2000): The Neogene Fonsdorf Basin: basin formation and basin inversion during lateral extrusion in the eastern Alps (Austria). Int. J. Earth Sci. 89, 415–430.

SASSI, F.P. and SCOLARI, A. (1974): The b_0 value of the potassium white micas as a barometric indicator in low-grade metamorphism of pelitic schists. Contrib. Mineral. Petrol. 45, 143–152.

SCHMIDT, D., LIVI, K.J.T. and FREY, M. (1999): Reaction progress in chloritic material: an electron microbeam study of the Taveyanne greywacke, Switzerland. J. Metamorphic Geol. 17, 229–241.

SCHMIDT, D., SCHMIDT, S.T., MULLIS, J., FERREIRO MÄHLMANN, R. and FREY, M. (1997): Very low-grade metamorphism of the Taveyanne formation of western Switzerland. Contrib. Mineral. Petrol. 129, 385–403.

SHAU, Y.H., PEACOR, D.R. and ESSENE, E.J. (1990): Corrensite and mixed-layer chlorite/corrensite in metabasalt from northern Taiwan: TEM/AEM, EMPA, XRD, and optical studies. Contrib. Mineral. Petrol. 105, 123–142.

STACH, E., MACKOWSKY, M.-T., TEICHMÜLLER, M., TAYLOR, G.H., CHANDRA, D. and TEICHMÜLLER, R. (1982): Coal Petrology. Gebrüder Bornträger, Berlin-Stuttgart, 535 pp.

THIELE, R. and MOREL, R. (1981): Tectonica Triásico-Jurásica en la Cordillera de la Costa, al norte y sur del Río Mataquito (34°45' – 35°15' Lat. S), Chile. Rev. Geol. Chile 13/14, 49–61.

VERGARA, M., LEVI, B. and VILLAROEL, R. (1993): Geothermal-type alteration in a burial metamorphosed volcanic pile, central Chile. J. Metamorphic Geol. 11, 449–454.

WARR, L.N., PRIMMER, T.J. and ROBINSON, D. (1991): Variscan very low-grade metamorphism in southwest England: a diastathermal and thrust-related origin. J. Metamorphic Geol. 9, 751–764.

WAPLES, D.W. (1980): Time and temperature in petroleum formations: Application of Lopatin's method to petroleum exploration. Bull. Am. Ass. Petro. Geol. 64, 916–929.

WOLF, M. (1975): Über die Beziehung zwischen Illit-Kristallinität und Inkohlung. N. Jb. Geol. Paläont. Mh. 7, 437–447.

Manuscript received December 14, 2001; revision accepted July 30, 2002.
Editorial handling: M. Engi